

## Supplementary information

### Adjustable electronic performances and redox ability of g-C<sub>3</sub>N<sub>4</sub> monolayer by absorbing nonmetal solute ions: A first principles study

S. Lu<sup>1</sup>, Z. W. Chen<sup>2</sup>, C. Li<sup>1\*</sup>, H. H. Li<sup>1</sup>, Y. F. Zhao<sup>1</sup>, Y. Y. Gong<sup>1</sup>, L. Y. Niu<sup>1</sup>, X. J. Liu<sup>1</sup> T. Wang<sup>3</sup> and C. Q. Sun<sup>1,4</sup>

<sup>1</sup> Center for Coordination Bond Engineering, College of Materials Science and Engineering, China Jiliang University, Hangzhou 310018, China

<sup>2</sup> Key Laboratory of Automobile Materials, Ministry of Education, Department of Materials Science and Engineering, Jilin University, Changchun 130022, China

<sup>3</sup> College of Electrical Engineering, Zhejiang University, Hangzhou 310027, China

<sup>4</sup> School of Electrical and Electronic Engineering, Nanyang Technological University, Singapore 639798

\*E-mail: [canli1983@gmail.com](mailto:canli1983@gmail.com)

Table S1. The wavelength of optical absorption edges  $\lambda_{\text{edge}}$  with unit nm. The integral area of optical absorption curves in ultraviolet ( $S_{\text{UV}}$ ) and visible light ( $S_{\text{V}}$ ) regions with uniform unit.

system	$\lambda_{\text{edge}}$		$S_{\text{UV}}$		$S_{\text{V}}$	
	2×2	3×3	2×2	3×3	2×2	3×3
pristine	455	461	626	558	216	205
H	462	455	619	601	152	129
B	449	447	608	578	237	205
C	449	445	610	585	200	191
Si	446	444	714	680	230	195
N	442	445	578	558	224	191
P	468	460	629	587	224	140
As	455	448	630	606	216	181
O	453	450	613	594	264	246
S	454	452	644	628	227	202
Se	458	454	635	609	199	162
Te	452	454	652	615	161	175
F	448	455	672	651	153	180
Cl	450	448	694	671	143	113
Br	458	451	701	682	143	110
I	453	449	702	680	144	117

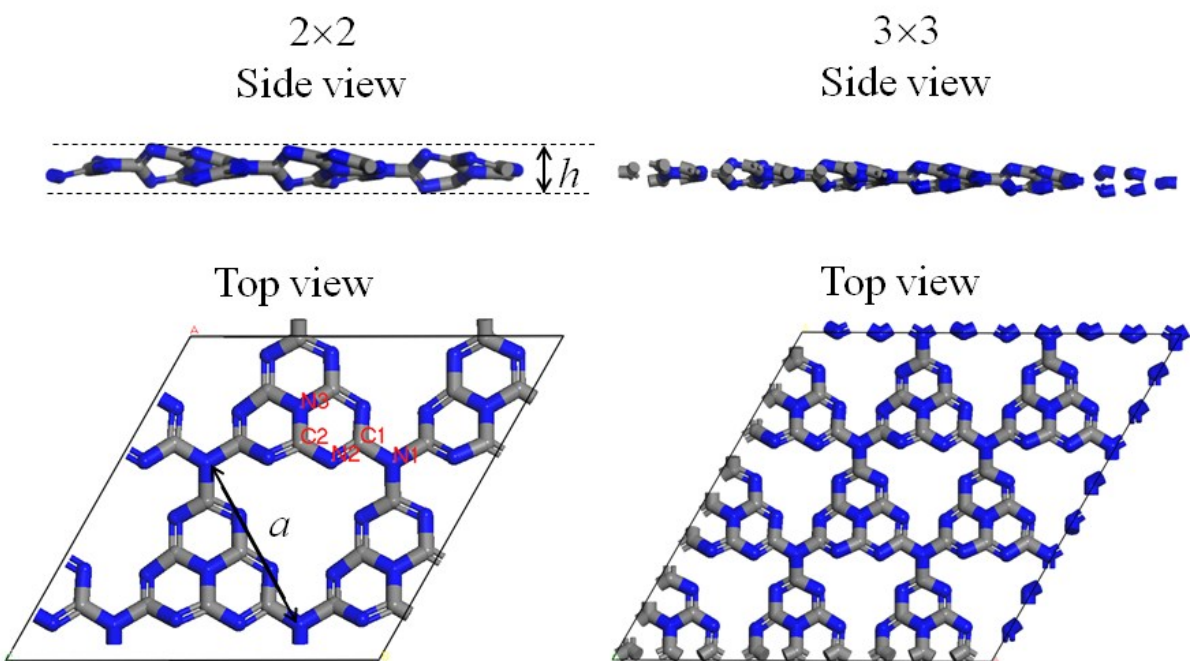


Figure S1. (Color online) Schematic structures of the  $2\times 2$  and  $3\times 3$  supercell g-C<sub>3</sub>N<sub>4</sub> monolayer, where the gray and blue spheres denote the C and N atoms.

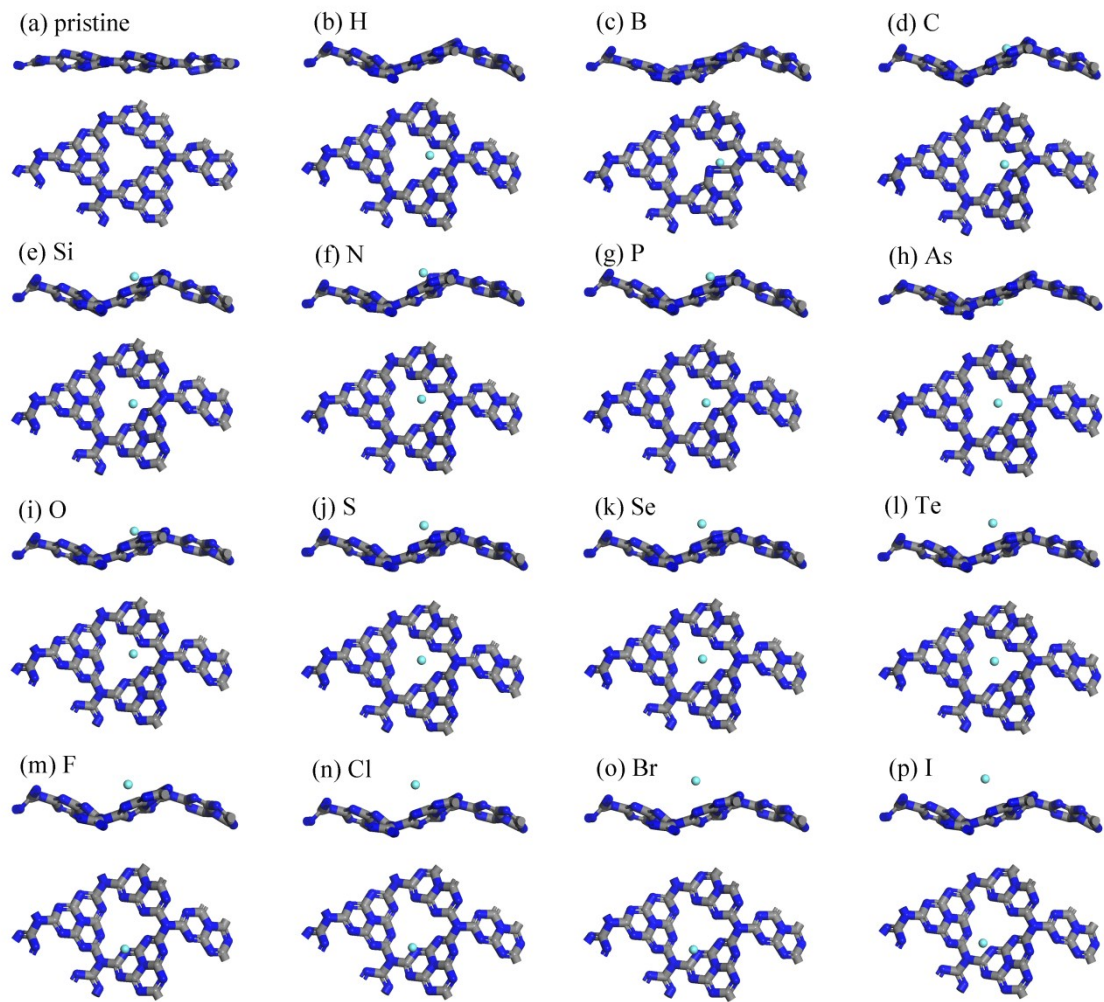


Figure S2. (Color online) The top and side views of (a)  $2\times 2$  pristine  $g\text{-C}_3\text{N}_4$  monolayer and (b-p) the  $g\text{-C}_3\text{N}_4$  monolayer after absorbing nonmetal atoms, where gray, blue and wathet spheres are the C, N and nonmetal atoms.

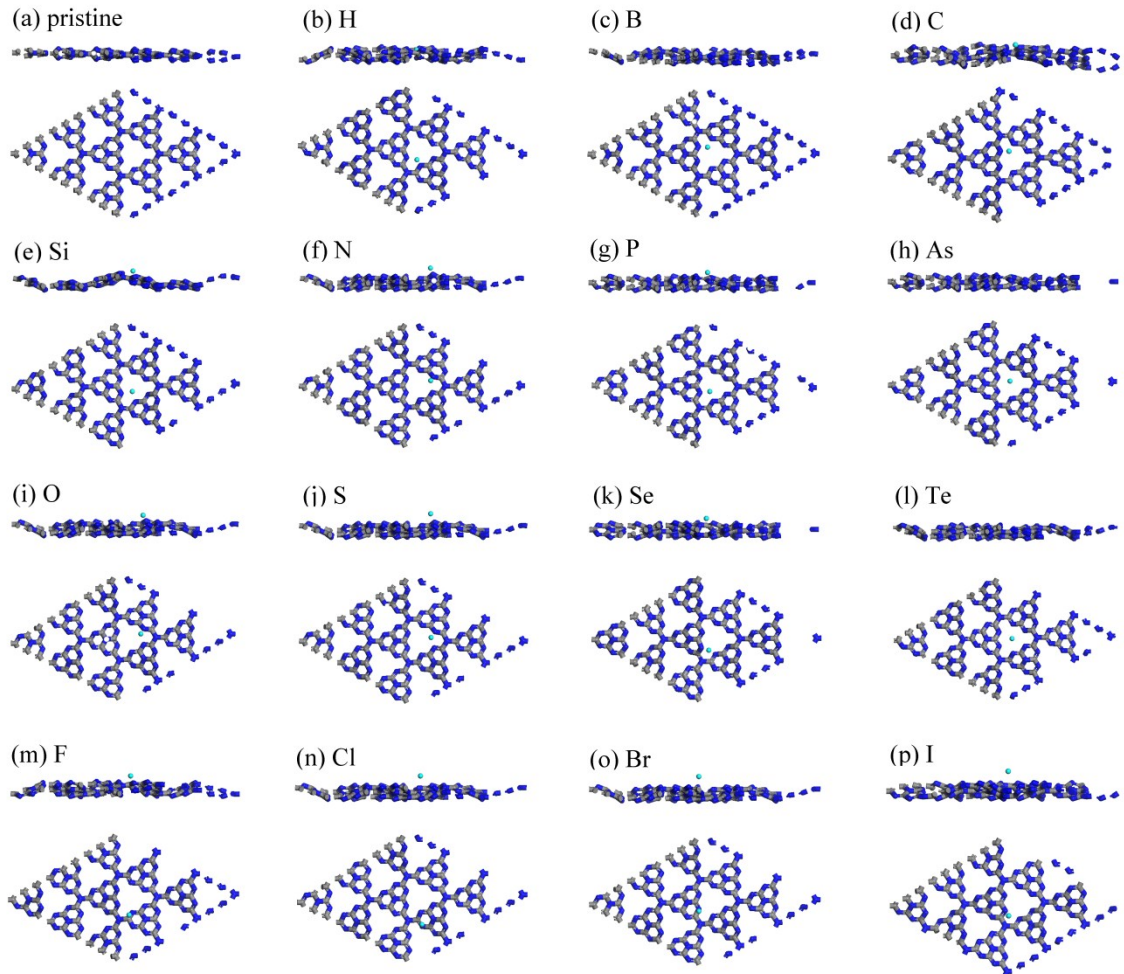


Figure S3. (Color online) The top and side views of (a)  $3 \times 3$  pristine  $\text{g-C}_3\text{N}_4$  monolayer and (b-p) the  $\text{g-C}_3\text{N}_4$  monolayer after absorbing nonmetal atoms, where gray, blue and wathet spheres are the C, N and nonmetal atoms.

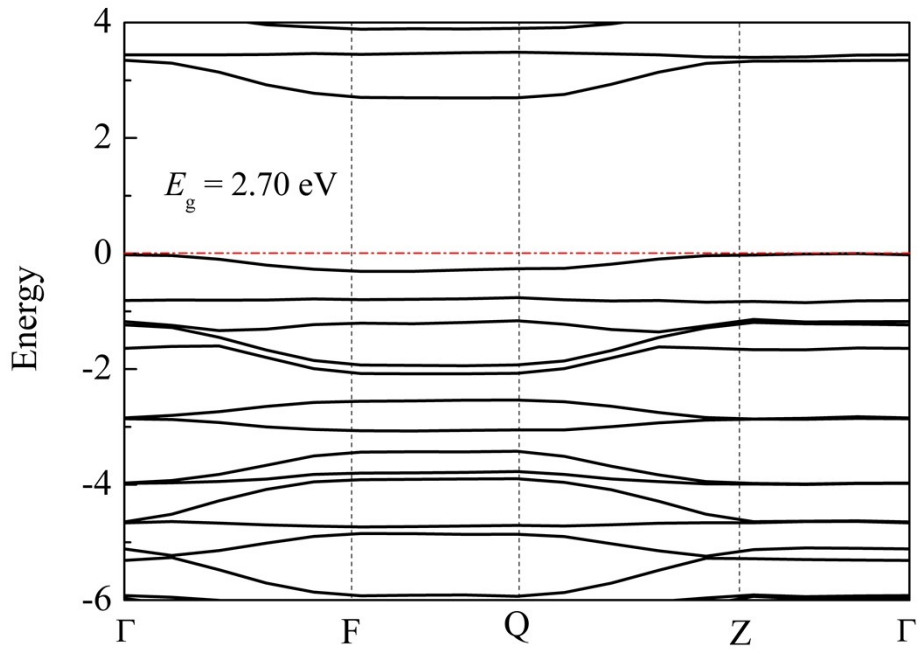


Figure S4. The band structure of pristine  $\text{g-C}_3\text{N}_4$  monolayer with hybrid functional.

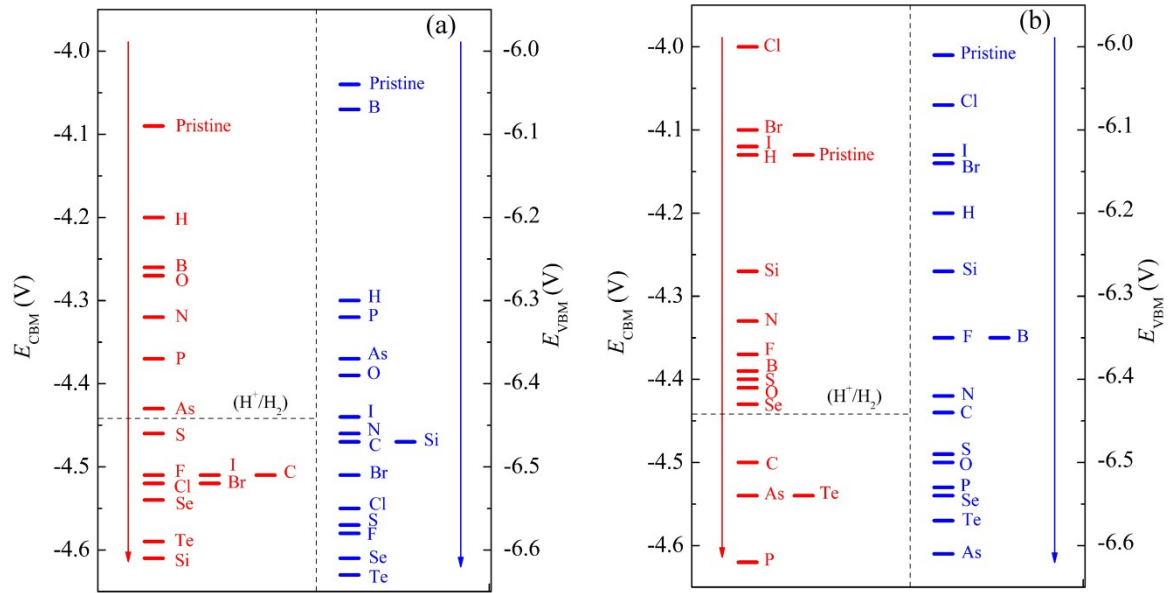


Figure S5. (Color online) The  $E_{CBM}$  and  $E_{VBM}$ , versus vacuum level of  $g\text{-C}_3\text{N}_4$  monolayer before and after absorbing nonmetal atom for (a)  $2\times 2$  and (b)  $3\times 3$  specimens.

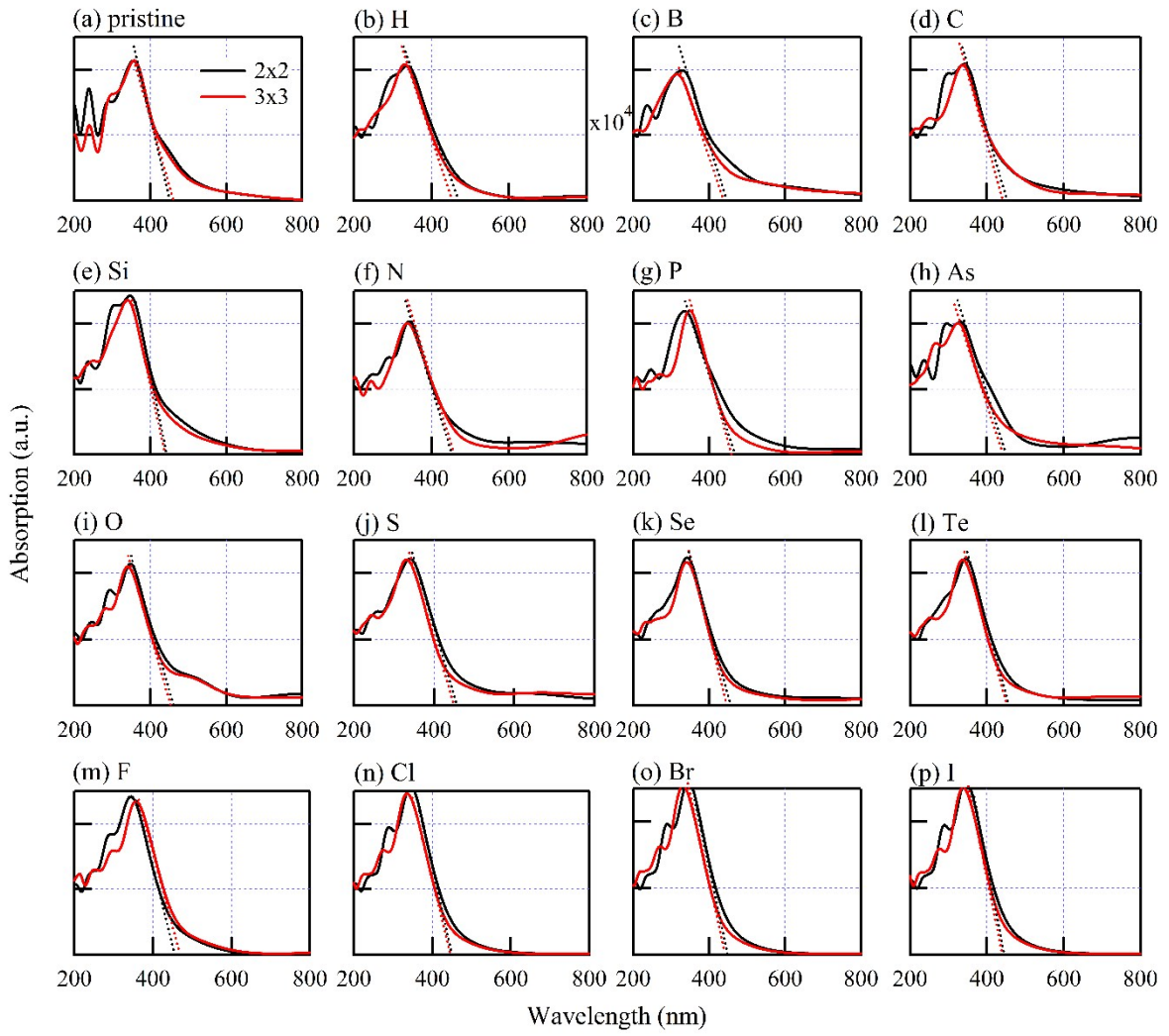


Figure S6. (Color online) The optical absorption curves of (a) pristine  $\text{g-C}_3\text{N}_4$  monolayer and (b-p)  $\text{g-C}_3\text{N}_4$  monolayer after absorbing nonmetal atoms for both  $2\times 2$  and  $3\times 3$  supercell specimens.